Science & Technology Development Journal 2024, 27(2):3463-3474

Open Access Full Text Article

Natural Sciences: Research article

Small-angle X-ray scattering analysis of ionic domain features in graft-type polymer electrolyte membranes

Nguyen Manh Tuan[1,2], Nguyen Huynh My Tue[1,2], Vo Thi Kim Yen[1,2], Nguyen Nhat Kim Ngan[2,3], Dinh Tran Trong Hieu[1,2], Hoang Anh Tuan[1,2], Doan Quoc Huy[1,2], Tran Duy Tap[1,2,*]

ABSTRACT

Introduction: Although poly(styrene sulfonic acid) (PSSA)-grafted poly(ethylene-co-tetrafluoroethylene) polymer electrolyte membranes (ETFE-PEMs) are potential polymer electrolyte membranes for fuel cells, there are only a few reports on the effect of synthesis steps and grafting degree (GD) on the features of ionic domains. These ionic features are related to the conductance and thus directly affect the fuel cell performance. Accordingly, this work reports SAXS analysis to determine the features of ionic domains, including domain sizes and interdomain distances, in ETFE-PEMs according to GDs. **Methods:** ETFE-PEMs were prepared via the irradiation of polystyrene onto the original ETFE matrix (grafted-ETFE) and subsequent sulfonation. The structural features of the ionic domains were investigated by the Ornstein–Zernike (OZ) and Teubner–Strey (TS) models based on the fitting of small-angle X-ray scattering (SAXS) profiles. **Results:** According to the OZ model, the polystyrene (PS) and PSSA grafts can be ordered up to 0.8 and 1.1 nm, respectively. Moreover, the TS model suggested that the interdomain distances of the PS and PSSA grafts were approximately 0.7 and 1.1 nm, respectively. **Conclusion:** The above SAXS results suggest that the grafted-ETFE films have the capacity for self-organization of graft domains. Moreover, phase separation occurred strongly at the sulfonation step, leading to the self-organization of ionic domains at larger dimensions compared to those of the corresponding graft layers.

Key words: Polymer electrolyte membrane, fuel cells, graft polymerization, SAXS

[1]*Faculty of Materials Science and Technology, University of Science, Ho Chi Minh City, 227 Nguyen Van Cu, District 5, Ho Chi Minh City, Vietnam*

[2]*Vietnam National University, Ho Chi Minh City, Vietnam*

[3]*Faculty of Physics and Engineering Physics, University of Science, Ho Chi Minh City, Vietnam*

Correspondence

Tran Duy Tap, Faculty of Materials Science and Technology, University of Science, Ho Chi Minh City, 227 Nguyen Van Cu, District 5, Ho Chi Minh City, Vietnam

Vietnam National University, Ho Chi Minh City, Vietnam

Email: tdtap@hcmus.edu.vn

History

- Received: 2024-04-12
- Accepted: 2024-05-31
- Published Online: 2024-6-30

DOI :

https://doi.org/10.32508/stdj.v27i2.4296

INTRODUCTION

Proton exchange membrane fuel cells (PEMFCs) are eco-friendly electrochemical devices with high conversion efficiency (~ 65%) that are suitable for transportation applications and portable devices [1,2]. There were 19,000 fuel cell electric vehicles (FCEVs) operating in the U.S., Japan, Europe, South Korea, and China as of 2019 [1]. The two most popular FCEVs at present are Hyundai Nexo and Toyota Mirai [1]. The polymer electrolyte membrane (PEM) is an important component of PEMFCs that directly affects fuel cell performance because of its proton conductance and ability to prevent gas diffusion through the PEM. Nafion is a commercial PEM, but it has low proton conductance at low relative humidity (RH) (< 50%) and high temperature (> 80 °C) and is expensive to produce [1,3]. This has motivated researchers to find alternative PEMs with suitable electrochemical properties at a reasonable price.

Recently, poly(styrene sulfonic acid) (PSSA)-grafted poly(ethylene-co-tetrafluoroethylene) (ETFE) polymer electrolyte membranes (ETFE-PEMs) have emerged as potential PEMs because some of the performance parameters of ETFE-PEMs are comparable to or better than those of conventional Nafion membranes [3,4]. The ETFE-PEMs were prepared by irradiating polystyrene onto the ETFE matrix to obtain the polystyrene-grafted ETFE (grafted-ETFE) and then performing sulfonation on the grafted film [3–13]. This process allows us to introduce a large amount of sulfonic acid groups to the ETFE matrix to form proton conductive channels while retaining useful properties, such as thermal stability and mechanical strength, of the original films [3,5]. The features of the ETFE-PEMs were studied in detail using different approaches, such as Fourier transform infrared (FT-IR) spectroscopy [14,15], positron annihilation lifetime spectroscopy [16,17], small-angle X-ray scattering (SAXS) [17–19], tensile strength [20], and X-ray photoelectron spectroscopy (XPS) [21]. Among these methods, SAXS is the most suitable approach for examining the microstructures and phase features of PEMs at different scales at the same time (the same SAXS profiles). Some works (using SAXS analysis) have reported the high-order microstructures of ETFE-PEMs, including the sizes

Cite this article : Tuan N M, Tue N H M, Yen V T K, Ngan N N K, Hieu D T T, Tuan H A, Huy D Q, Tap T D. **Small-angle X-ray scattering analysis of ionic domain features in graft-type polymer electrolyte membranes**. *Sci. Tech. Dev. J.* 2024; 27(2):3463-3474.

and interdomain distances of ionic layers with large dimensions[3–13]. These ionic domains have clear phase separation with the hydrophobic polymer backbone and are related directly to the conductance of membranes[13,22]. However, there are only a few reports on ionic layers at low dimensions (subnano- to nanolevels)[8,13]. In the graft-type PEM system, a water channel is expected to be created around the ionic domains[15]. Accordingly, the structural parameters of ionic domains are necessary to understand the structure-conductance relationship, which can control the PEM performance in PEMFCs.

The ionic domain sizes and interdomain distances of PEMs have been studied by the analysis of small-angle X-ray scattering (SAXS) profiles using Guinier[13], Debye-Bueche (DB)/combined with Teubner-Strey (TS)[23,24], and Ornstein-Zernike (OZ) models[25,26]. However, there have been no reports on the ionic domains of ETFE-PEMs using the OZ[25,26] and TS models[27–29], although these are effective approaches for determining the microstructural parameters of membranes. Accordingly, this study focuses on the domain sizes and interdomain distances of grafted-ETFE films and ETFE-PEMs using the OZ and TS models. The OZ and TS models were used for fitting the SAXS profiles because the OZ model is suitable for describing the correlation length or domain size of inhomogeneity systems[25,26], while the TS model is suitable for extracting structural information from two immiscible phase systems[27–29]. Similar to OZ, the Guinier[30] and DB[31] models are also utilized to determine the correlation length or domain size in the above films and membranes for comparison.

EXPERIMENTAL

Materials and ETFE-PEM preparation

The original ETFE films (50 mm in thickness) were purchased from Asahi Glass Co. Ltd., Japan. The ETFE-PEMs were prepared using the same synthetic process described in a previous study[3]. The synthetic procedure is shown in Scheme 1. A Co^{60} gamma radiation source with an absorbed dose of 15 kGy under an argon atmosphere was used for irradiating polystyrene onto the original ETFE films to create polystyrene-grafted ETFE (grafted-ETFE) films. The grafting degree (GD) is determined as the percentage of the grafting polymer weight and the original film weight: GD(%) = 100(Wg -Wo)/Wo. Here, Wg and Wo are the weights of the grafted-ETFE film and the pristine film, respectively. The original ETFE film was cut to a size of 6x8 cm^2 and weighed prior to the irradiation process. After grafting with polystyrene solution, the surface of the grafted ETFE film was cleaned to remove the homopolymer and the residual monomers prior to weight measurement. In this work, the GD was controlled by varying the monomer concentration and grafting time while maintaining other conditions of irradiation and grafting, such as the irradiation dose, temperature, and solvent. Finally, the grafted-ETFE films were immersed in 0.2 M chlorosulfonic acid solution at 50 °C for 6 hours for sulfonation to obtain the ETFE-PEMs.

SAXS measurements

Scheme 2 illustrates the SAXS measurements. The SAXS profiles were measured at room temperature and 60% relative humidity using Mo-Kα radiation (wavelength, l = 0.07 nm) (Rigaku NANO-Viewer, Japan) at the National Institute of Material Science (NIMS) in Japan. The sample-detector distance was 35 cm. The Q-range of the SAXS profiles was Q = 1.0–10.0 nm^{-1}. Here, Q is the magnitude of the scattering momentum transfer, equaling $4\pi \sin(\theta)/\lambda$, where 2θ is the scattering angle and λ is the incident X-ray wavelength. The scattering intensities were circularly averaged and corrected using the secondary standard of glassy carbon (provided by Argonne National Laboratory, USA) to obtain the absolute intensities[5,32]. More details on the SAXS measurements can be found in our previous work[5].

SAXS analysis

In our previous works[9,13], field emission scanning electron microscopy (FE-SEM) measurements showed that ionic domains have different sizes/shapes. Moreover, PSSA chains were not mixed with the amorphous phase of the ETFE matrix, leading to membranes having two immiscible phase systems[12,21]. Therefore, the OZ model (suitable for describing inhomogeneity systems)[25,26] and TS model (suitable for describing two immiscible phase systems)[27–29] were used in this work. To enrich the results, we modeled the morphology of the ionic domains using the popular Guinier[30] and DB[31] models. Similar to the OZ model, the Guinier and DB models are suitable for studying inhomogeneity systems[30,31].

OZ model

The OZ model is applicable for describing material regions with random shapes[25,26] and is suitable for extracting the sizes of grafted polystyrene layers of grafted ETFE films and the ionic domains of ETFE-PEMs. According to OZ theory[25,26], the scattering

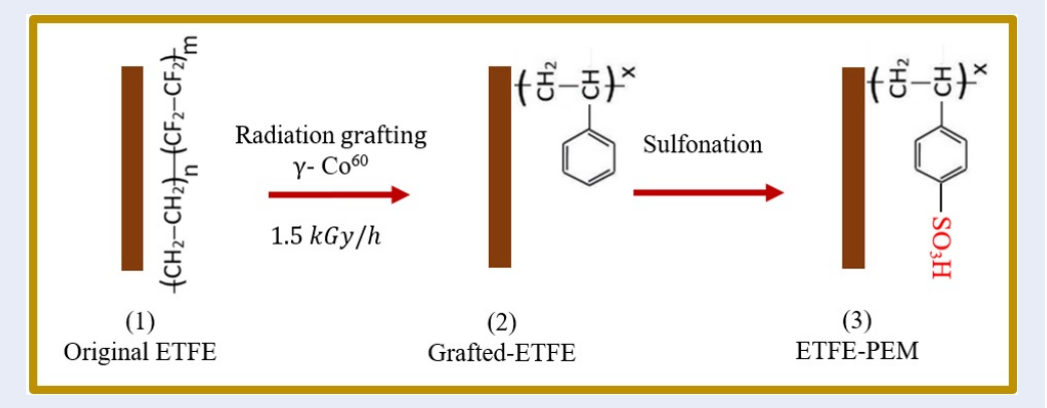

Scheme 1: Synthetic process and chemical structures of ETFE, grafted-ETFE, and ETFE-PEM.

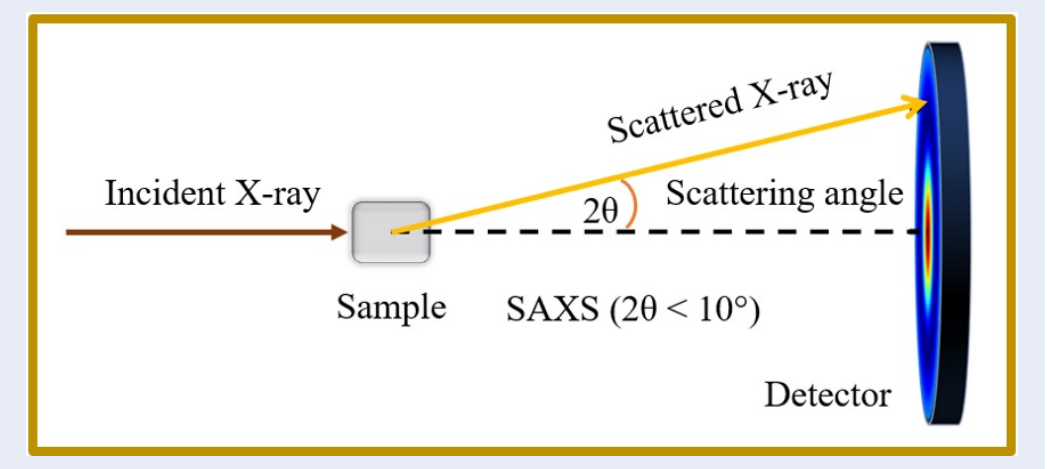

Scheme 2: Illustration of the SAXS measurements.

intensity near Q = 0 is given by:

$$I_{OZ}(q) = \frac{I_{OZ}(0)}{1 + \zeta_{OZ}^2 \cdot q^2} \quad (1)$$

where ζ_{OZ} is the correlation length or domain size and $I_{OZ}(0)$ is the scattering intensity at Q = 0. The fitting parameters follow the least square law. The fitting was performed at least four times, and the fitting parameters were averaged. A similar fitting procedure was also applied to the Guinier, DB, and TS models. Table 1 shows the averaged fitting parameters of the OZ, Guinier, and DB models to compare the results of domain sizes using different models, while Table 2 shows those of the TS models to discuss interdomain distances.

Guinier model

In 1939, Guinier proposed an approximation equation to determine the radius of gyration R_g for samples with solid spherical molecules as well as ionomers[30]. The radius of gyration is the square root of the average squared distance of each scatterer from the particle center. This size is not fixed for objects with the same volume but different shapes. According to Guinier theory[30], the scattering intensity near Q = 0 is given by:

$$I_g(q) = I_g(0)\, exp\left(-\frac{1}{3}q^2 R_g^2\right) \quad (2)$$

where $I_g(0)$ is the scattering intensity at Q = 0.

DB model

The DB model is used to determine the correlation length or domain size of inhomogeneous systems. The Debye-Bueche model is suitable for determining these structural parameters in a sharp two-phase system, where both the sizes and shapes of the phases are random. This model follows an exponential decay of

the electron density correlation function. The relevant expression from this model is as follows[31]:

$$I_{DB}(q) = \frac{A^2}{\left(1+\zeta_{DB}^2 q^2\right)^2} \quad (3)$$

where A depends on the system in question and ζ_{DB} is called the correlation length or domain size.

TS model

The TS model is applicable for describing two-phase systems with distinct boundaries and has been used for the intermeshing of hydrophobic and hydrophilic structures when the particle shape is not well defined[27–29]. In this case, the clear phase separation of ionic regions and the ETFE backbone was described in a previous study[22]. In the TS model, the pair correlation function γ(r) in real space is assumed to have the following form:

$$\gamma(r) = \frac{d_{TS}}{2\pi r} exp\left(-\frac{r}{\xi_{TS}}\right) \sin\left(\frac{2\pi r}{d_{TS}}\right) \quad (4)$$

where d_{TS} is the domain periodicity or interdomain distance and ξ_{TS} is a correlation length that has been attributed to the dispersion of d_{TS}. Then, the scattering intensity profile, I_{TS}(q), can be expressed as follows:

$$I_{TS}(q) = \frac{1}{a_2 + c_1 q^2 + c_2 q^4} \quad (5)$$

where $a_2 > 0$, $c_1 < 0$, and $c_2 > 0$. The TS model is suitable for a single broad scattering maximum and a power law decay of –4 at large scattering angles. Furthermore, a_2, c_1, and c_2 are also parameters used to fit one-dimensional SAXS profiles and can also be used to calculate the correlation length (ξ_{TS}) and domain spacing (d_{TS}) via the following equations:

$$\xi_{TS} = \left[\frac{1}{2}\left(\frac{a_2}{c_2}\right)^{1/2} + \frac{c_1}{4c_2}\right]^{-1/2} \quad (6)$$

$$d_{TS} = 2\pi\left[\frac{1}{2}\left(\frac{a_2}{c_2}\right)^{1/2} - \frac{c_1}{4c_2}\right]^{-1/2} \quad (7)$$

The fitting of the SAXS profiles using equation (5) was performed to extract the structure parameters and pair correlation function.

RESULTS

The plots of the best-fit OZ models for the SAXS profiles of the grafted-ETFE films with GDs of 36 and 61% are shown in Figure 1a,b. The OZ models (orange lines) are plotted by the fitting regions with a Q-range of 2.0–3.5 nm^{-1}. A screening process was carried out to determine good fitting regions as good as the suitable fitting parameters of $I_{OZ}(0)$ and ζ_{OZ}. The suitable region for fitting is between the ionic peak and the Porod region [5,7,8]. In this work, several Q-regions are selected for the fitting process, and the fitting parameters of $I_{OZ}(0)$ and ζ_{OZ} are averaged. This procedure is applied similarly for the Guinier, DB, and TS models. The grafted polystyrene domain sizes of the grafted ETFEs (with GDs of 36 and 61%) are approximately 0.78 nm. Figure 1c,d shows the plots of the Guinier models for the SAXS profiles of the similar films. The Guinier models (green lines) are plotted by the fitting regions with a Q-range of 1.9–2.8 nm^{-1}. The grafted polystyrene domain sizes extracted from the Guinier model were also nearly 0.78 nm. The plots of the DB models are shown in Figure 1e,f. The pink lines represent the DB models with the fitting regions having a Q-range of 1.2–2.7 nm^{-1}. The grafted polystyrene domain sizes extracted from the DB model can be ordered up to approximately 0.80 nm. The structural parameters extracted from each model are shown in Table 1.

A similar fitting procedure was applied for the SAXS profiles of the ETFE-PEMs with GDs of 36 and 61%. Figure 2a,b illustrates the best-fitting OZ model for the SAXS profiles of the ETFE-PEMs. The fitting regions have a Q-range of 1.5–2.5 nm^{-1}. The ionic domain sizes extracted from the OZ model are approximately 1.07 nm. The plots of the Guinier model for fitting the SAXS profiles of the ETFE-PEMs are shown in Figure 2c,d. The Guinier model was applied for the region with a Q-range of 1.3–2.0 nm^{-1}. The results of the Guinier model still show that the ionic domains can be ordered up to 1.12 nm. The plots of the DB model are shown in Figure 2e,f. The fitting regions have a Q-range of 0.9–1.7 nm^{-1}. Similar to the results of the OZ and Guinier models, the domain sizes extracted from the DB model are approximately 1.11 nm. The structural parameters extracted from each model are shown in Table 1.

Figure 3a,b shows the plots of the TS model for fitting the SAXS profiles of the grafted ETFEs with a GD of 36% and the related correlation (gamma) function γ(r). This model was applied for fitting a peak with a Q-range of 4.2–8.4 nm^{-1}. In this case, the TS model allows us to extract the correlation distance between grafted polystyrene domains of nearly 0.71 nm. The correlation function shows an intensive peak at 0.8 nm and further peaks at approximately 1.6 and 2.3 nm. These peaks represent the correlation distances between grafted polystyrene domains. The plots of the best-fitting TS model and the related correlation function of the grafted ETFE with a GD of 61% are shown

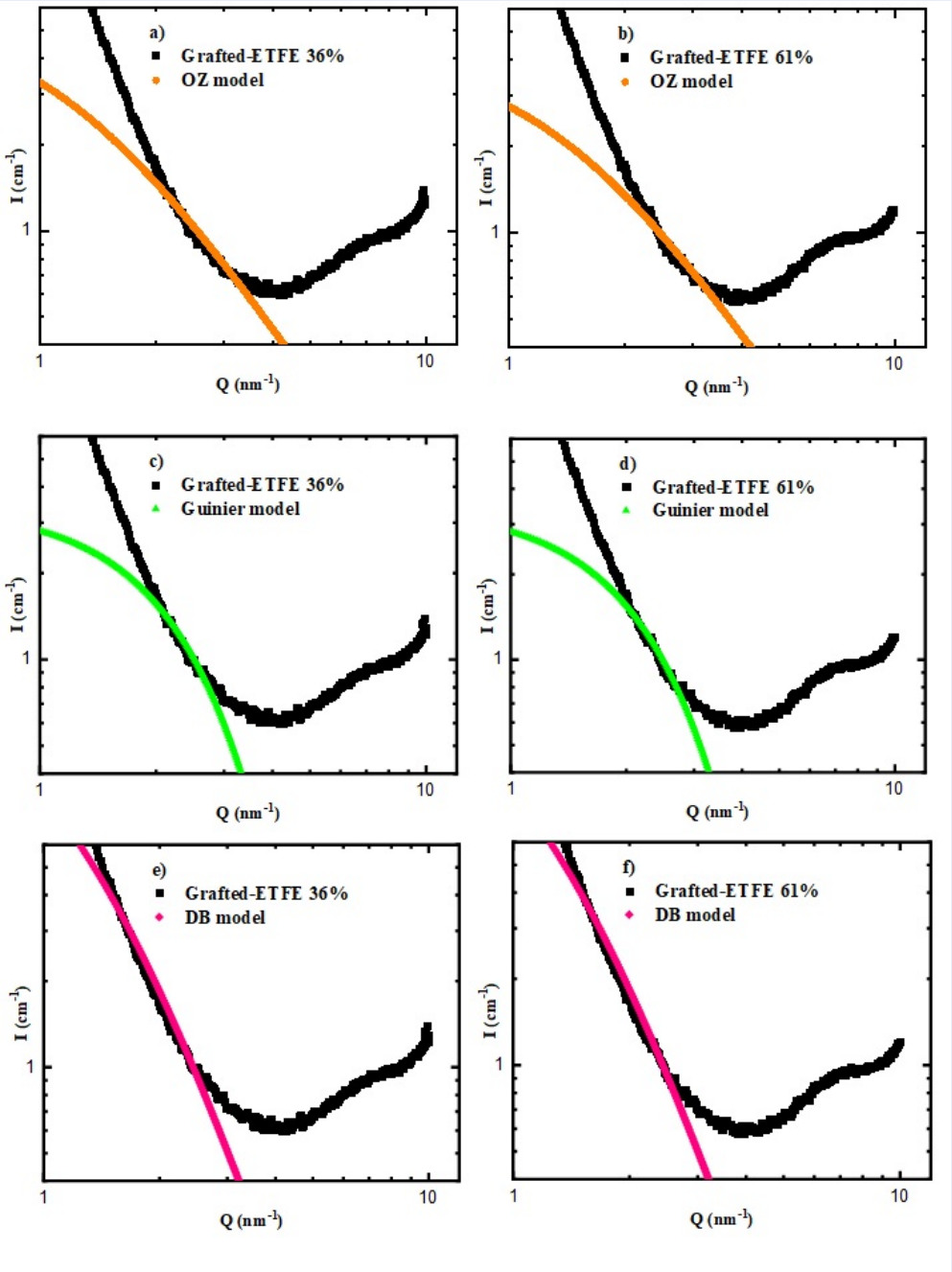

Figure 1: The plots of OZ, Guinier, and DB model fitting for the SAXS profiles of grafted-ETFE films with GDs of 36 and 61%. The fitting is conducted in several Q-ranges and the obtained fitting parameters are averaged. The fitting parameters are represented in Table 1.

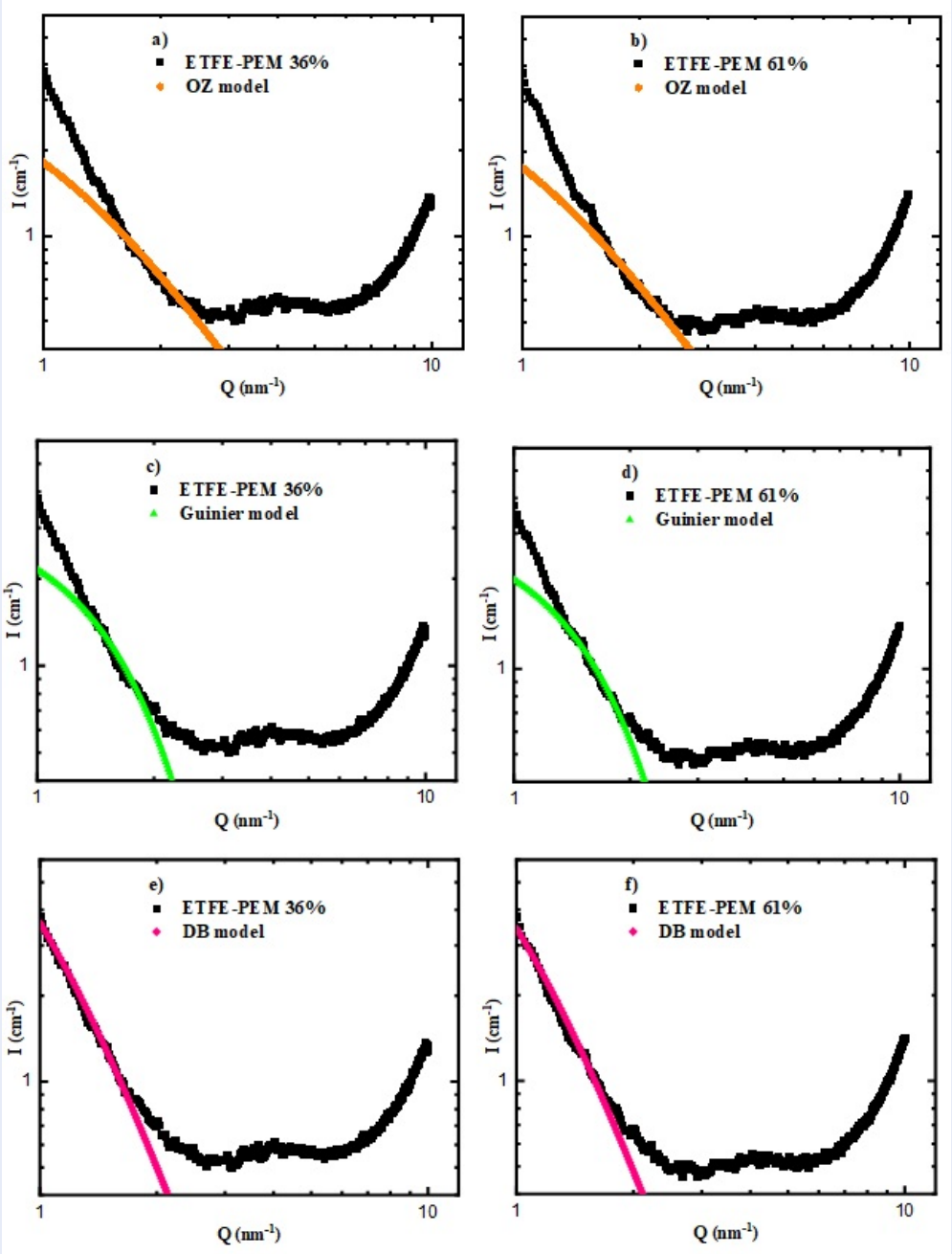

Figure 2: The plots of OZ, Guinier, and DB model fitting for the SAXS profiles of the ETFE-PEMs with GDs of 36 and 61%. The fitting is conducted in several Q-ranges and the obtained fitting parameters are averaged. The fitting parameters are represented in Table 1.

Table 1: Domain sizes were extracted from fitting for the SAXS profiles using the OZ, Guinier, and DB models of grafted-ETFE films and the ETFE-PEMs having GDs of 36 and 61% and compared with those of other membranes

Sample	Microstructures	Model	Domain size (nm)	Ref
Grafted-ETFE 36%	Grafted polystyrene domain	OZ	0.78 ± 0.05	This study
		Guinier	0.77 ± 0.01	
		DB	0.80 ± 0.01	
Grafted-ETFE 61%	Grafted polystyrene domain	OZ	0.77 ± 0.03	This study
		Guinier	0.77 ± 0.01	
		DB	0.81 ± 0.01	
ETFE-PEM 36%	Ionic domain	OZ	1.07 ± 0.06	This study
		Guinier	1.12 ± 0.01	
		DB	1.11 ± 0.01	
ETFE-PEM 61%	Ionic domain	OZ	1.15 ± 0.05	This study
		Guinier	1.14 ± 0.01	
		DB	1.11 ± 0.01	
Poly(ethylene oxide)-block-poly((vinyl benzyl)trimethylammonium chloride)	Hard phase	OZ	≈ 3.8–5.9	[26]
Poly(N-isopropyl acrylamide) (pNIPAAm)	Polymer-network mesh size	OZ	≈ 1.0–10	[33]
Nafion	The packing of two aligned backbones	OZ	≈ 0.5–0.7	[34]

in Figure 3c,d. The fitting region has a Q-range of 4.2–8.6 nm^{-1}. The results from the TS model show that the intergrafted polystyrene domains are nearly 0.74 nm in length. The derived correlation function shows the first, second, and third peaks at approximately 0.9, 1.7, and 2.7 nm, respectively. The fitting results can be seen in Table 2.

Figure 4a,b shows the plots of the best-fitting TS model for the SAXS profiles of ETFE-PEM (GD = 36%) and the derived correlation function $\gamma(r)$. The fitting region has a Q-range of 2.7–5.5 nm^{-1}. In this case, the correlation distance between the ionic domains extracted from the TS model is approximately 1.13 nm. The relative correlation function shows an intense peak at 1.2 nm and a further peak at approximately 2.4 nm. The plots of the TS model and related correlation function of ETFE-PEM (GD = 61%) are shown in Figure 4c,d. The fitting by the TS model was applied for the region with a Q-range of 2.8–5.7 nm^{-1}. The interionic domain distance is approximately 1.06 nm. The derived correlation function shows the first peak at 1.2 nm and the second peak at nearly 2.3 nm. The fitting results can be seen in Table 2.

The above results of SAXS analysis indicate that four models, OZ, Guinier, DB, and TS, are applicable for the ionic domains of ETFE-PEMs. The TS model requires the SAXS peak for fitting, while this is not necessary for the OZ, Guinier, and DB models. The fitting results presented in Table 1 and Table 2 lead to the conclusion that the domain size and domain distance of the ionic aggregates are independent of the GD. However, increasing the number of ionic groups according to GD should improve the proton conductance[15]. The results shown in Table 2 suggest that the domain distances in the ETFE-PEMs are lower than those in the other PEMs[35–37]. In other words, the ionic groups in the ETFE-PEMs are more densely aggregated.

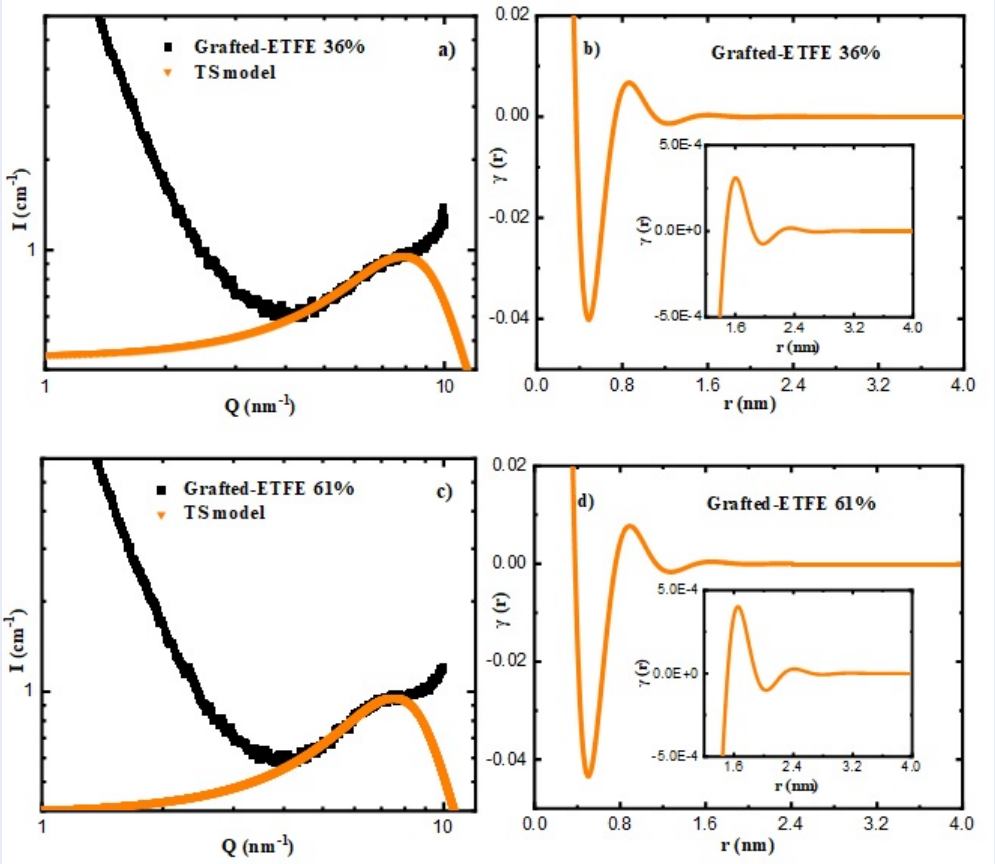

Figure 3: Plots of the TS model and derived gamma function of the grafted ETFE films: a, b) with a GD of 36%; c, d) with a GD of 61%. The fitting is conducted in several Q-ranges and the obtained fitting parameters are averaged. The fitting parameters are represented in Table 2.

Table 2: Domain distances extracted from the TS model of the grafted-ETFE films and the ETFE-PEMs with GDs of 36 and 61% and compared with those of other membranes

Sample	Microstructures	Domain distance (nm)	Ref
Grafted-ETFE 36%	Grafted polystyrene domain	0.71 ± 0.01	This study
Grafted-ETFE 61%	Grafted polystyrene domain	0.74 ± 0.01	This study
ETFE-PEM 36%	Ionic domain	1.13 ± 0.01	This study
ETFE-PEM 61%	Ionic domain	1.06 ± 0.02	This study
Polyimide and poly(ethylene glycol) doped with an ionic liquid	Ionic liquid	≈ 9.0–15.0	[35]
Sulfonated polyphenylenes composed of m- and p-phenylene groups with sulfonic acid substituents (SPP-QP).	Hydrophilic domain	≈ 7.0–8.0	[36]
ETFE-PEM cross-linked with 1,3-diisopropenylbenzene	Ionic domain	≈ 1.5	[37]

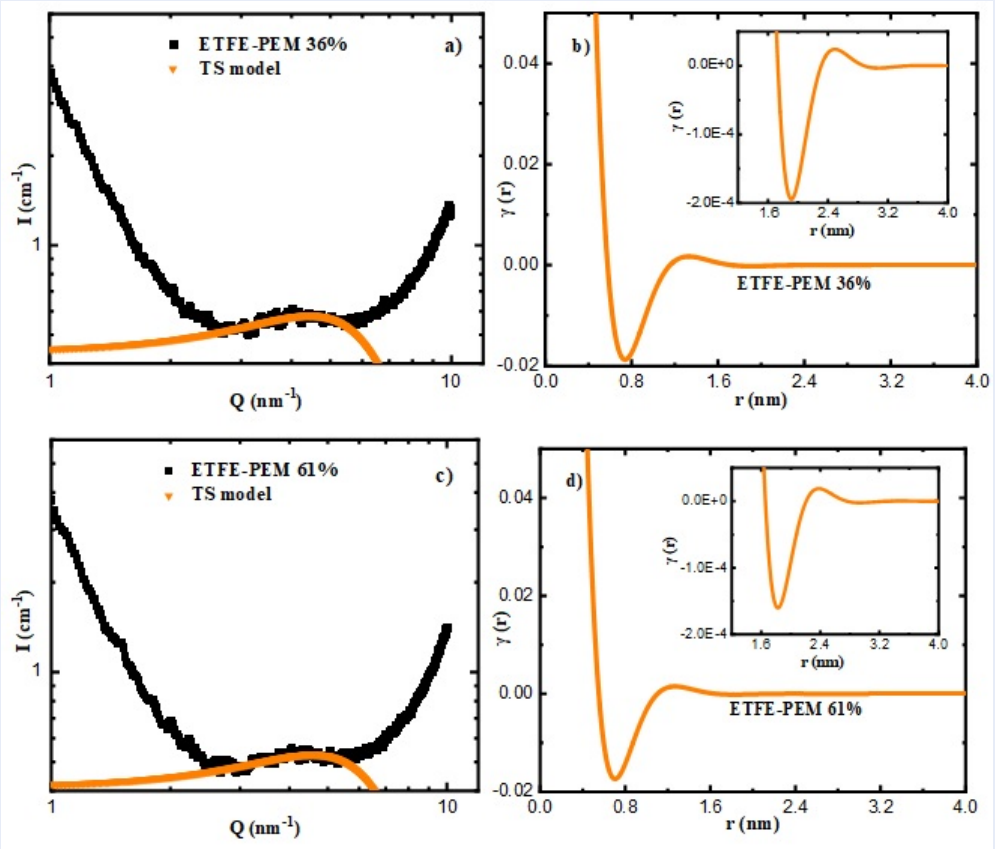

Figure 4: Plots of the TS model and derived gamma function of the ETFE-PEMs: a, b) with a GD of 36%; c, d) with a GD of 61%. The fitting is conducted in several Q-ranges and the obtained fitting parameters are averaged. The fitting parameters are represented in Table 2.

DISCUSSION

The domain sizes of the polystyrene grafts extracted from the OZ, Guinier, and DB models for the grafted-ETFE films with GDs of 36% (0.78–0.80 nm) and 61% (0.77–0.81 nm) are highly similar. A similar case is true for the ETFE-PEMs with GDs of 36% (1.07–1.12 nm) and 61% (1.11–1.15 nm). In other words, the domain sizes at the different GDs (36% and 61%) of both the grafted-ETFE film and the ETFE-PEMs are similar. This result indicates that the grafted-ETFE films and the ETFE-PEMs can accommodate more PS and PSSA chains with small changes in their domain sizes[13]. The ionic domain sizes of the ETFE-PEMs are greater than those of the corresponding polystyrene graft domain sizes. This result can be attributed to the phase separation of PSSA grafts from the backbones of the ETFE matrix at the sulfonation step[13]. These PSSA grafts can be connected, aggregated, and shelf-organized to form ionic domains. As reported previously[13,23,24], the structural features of these ionic domains, including domain sizes, strongly affect the conductance of membranes for fuel cells. For example, the conductance of ETFE-PEM (GD = 34%) is 5 times greater than that at GD = 19%. This significant increase in conductance was elucidated by the short-range distances of the ordered ionic nanochannels, which allowed the creation of water channels. These water channels are favorable for high proton conductance even at low relative humidity[13]. The domain sizes extracted from the OZ model for poly(ethylene oxide)-block-poly((vinyl benzyl)trimethyl-ammonium chloride) (3.8–5.9 nm)[26], poly(N-isopropyl acrylamide) (pNIPAAm) (1–10 nm)[33], and Nafion (0.5–0.7 nm)[34] are shown in Table 1 for comparison. In this case, the domain sizes of polystyrene grafts are greater than those of the packing of two aligned backbones of Nafion membranes.

The TS model allows us to describe a system with clear phase separation with interdomain distances of approximately 0.7 and 1.1 nm for grafted polystyrene

domains and ionic domains, respectively. In addition, the derived correlation function shows that the nearest correlation distances of the grafted polystyrene domains and ionic domains are approximately 0.8 and 1.2 nm, respectively. As shown in Tables 1 and 2, the change in structural parameters determined from the TS model did not vary with GD, as determined by the OZ, Guinier, and DB models for both the grafted-ETFE films and the ETFE-PEMs[13]. In addition, the peak features observed in the plots of the TS model (Figure 3 and Figure 4) provide further information on the size distribution of ionic domains, which could not be obtained by the OZ, Guinier, and DB models. Accordingly, the TS model is the most suitable approach for observing the ionic domains of ETFE-PEMs. The structural parameters extracted from the TS model for polyimide and poly(ethylene glycol) doped with an ionic liquid (9–15 nm)[35], sulfonated polyphenylenes composed of m- and p-phenylene groups with sulfonic acid substituents (SPP-QP) (7–8 nm)[36], and ETFE-PEM cross-linked with 1,3-diisopropenylbenzene (1.5 nm)[37] are shown in Table 2 for comparison. The domain distances of the ETFE-PEMs are lower than those of the ETFE-PEMs cross-linked with 1,3-diisopropenylbenzene. This result suggested that the aggregation and concentration of PSSA grafts are hindered by cross-linking with 1,3-diisopropenylbenzene. The obtained results in Tables 1 and 2 indicate that the domain sizes and interionic domain distances of the ETFE-PEMs can be controlled at irradiation grafting step[13]. Based on the results of the fitting models, we propose a model for the microstructural features of ETFE-PEM consisting of PS and PSSA graft domains (Figure 5).

The above results indicate that the simultaneous application of the OZ, Guinier, DB and TS models is necessary to evaluate both the domain sizes and distances of the ionic domains. However, as shown in Figure 1 and Figure 2, the fitting is only applied in the limited Q-range for the case of the OZ and Guinier models. Further evaluation of the features of the ionic domains in the ETFE-PEMs at lower and higher GDs using SAXS analysis is necessary to understand the structure-conductance relation.

CONCLUSIONS

The domain sizes and interdomain distances of the PS and PSSA grafts of the grafted-ETFE films (~ 0.8 nm) and the ETFE-PEMs (~ 1.1 nm) were determined by the OZ and TS models and compared to those of the Guinier and DB models via SAXS profile fitting. The domain sizes and interdomain distances did not vary with GDs of 36 and 61%, respectively, indicating that both the grafted films and membranes can accommodate more PS and PSSA chains with small changes in their dimensions. The ionic domain sizes of the ETFE-PEMs can be controlled at the irradiation grafting step. The ionic domain sizes of the ETFE-PEMs were greater than the corresponding polystyrene graft domain sizes of the grafted ETFE films, which can be explained by the phase separation of the PSSA grafts from the backbones of the ETFE matrix at the sulfonation step. Note that the PSSA grafts in the ETFE-PEMs can be connected, aggregated, and shelf-organized to form ionic domains at low dimensions, which is much lower than those in the ETFE-PEMs cross-linked with 1,3-diisopropenylbenzene (~ 1.5 nm) and commercial Nafion membranes (2–5 nm). The features of the ionic domains of the ETFE-PEMs under various RH conditions are progressing.

ACKNOWLEDGMENTS

This research is funded by the Vietnam National Foundation for Science and Technology Development (NAFOSTED) under grant number 103.99-2020.59.

LIST OF ABBREVIATIONS

DB: Debye-Bueche
ETFE: Poly(ethylene-co-tetrafluoroethylene)
ETFE-PEMs: Poly(styrene sulfonic acid) (PSSA)-grafted poly(ethylene-co-tetrafluoroethylene) (ETFE) polymer electrolyte membranes
FCEV: Fuel cell electric vehicles
FT-IR: Fourier transform infrared
GD: Grafting degree
grafted-ETFE: Polystyrene-grafted ETFE
NIMS: National Institute of Material Science
OZ: Ornstein-Zernike
PEM: Polymer electrolyte membrane
PEMFCs: Proton exchange membrane fuel cells
pNIPAAm: Poly(N-isopropyl acrylamide)
PS: Polystyrene
PSSA: Poly(styrene sulfonic acid)
RH: Relative humidity
SAXS: Small-angle X-ray scattering
SPP-QP: Sulfonated polyphenylenes composed of m- and p-phenylene groups with sulfonic acid substituents
TS: Teubner-Strey
XPS: X-ray photoelectron spectroscopy

CONFLICT OF INTEREST

The authors declare that they have no conflicts of interest.

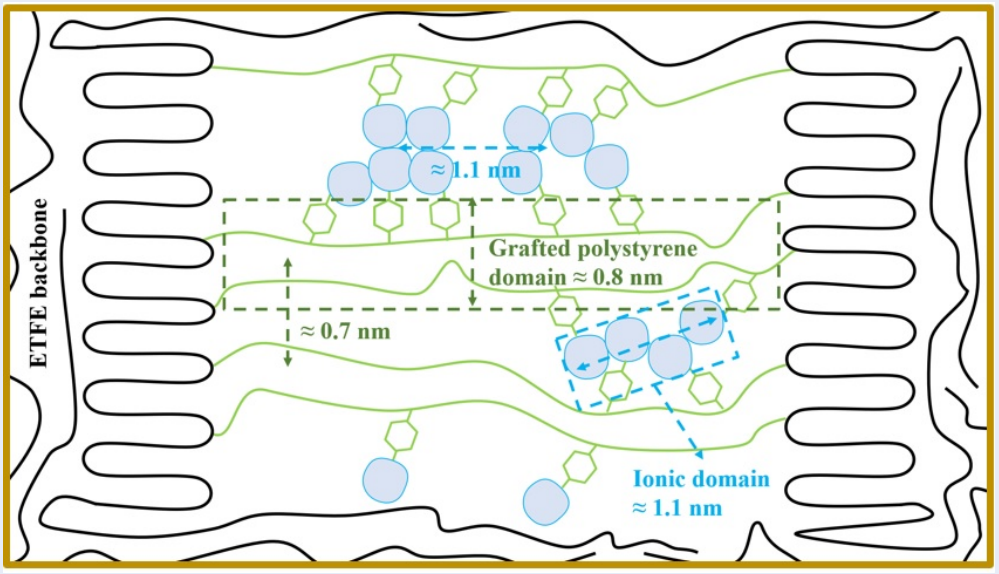

Figure 5: Illustration of the microstructures of ETFE-PEMs. Grafted polystyrene domains and ionic domains can organize at scales of 0.8 and 1.1 nm, respectively.

DATA AVAILABILITY STATEMENT

The data sets are not publicly available but are available from the corresponding author upon reasonable request.

AUTHORS CONTRIBUTION

Tran Duy Tap: Conceptualization, Project administration, Funding acquisition, Supervision, Resources, Investigation, Methodology, Data curation, Formal analysis, Supervision, Validation, Visualization, Writing - original draft, Writing - review & editing. **Nguyen Manh Tuan:** Investigation, Methodology, Data curation, Formal analysis, Validation, Visualization, Writing - original draft, Writing - review & editing. **Nguyen Huynh My Tue**, **Vo Thi Kim Yen**, **Nguyen Nhat Kim Ngan**, **Dinh Tran Trong Hieu**, **Hoang Anh Tuan**, **Doan Quoc Huy:** Visualization, Validation, Writing- review & editing.

REFERENCES

1. Wang Y, Seo B, Wang B, Zamel N, Jiao K, Adroher XC. Fundamentals, materials, and machine learning of polymer electrolyte membrane fuel cell technology. Energy AI. 2020;1:100014;Available from: https://doi.org/10.1016/j.egyai.2020.100014.
2. Nasef MM. Radiation-grafted membranes for polymer electrolyte fuel cells: current trends and future directions. Chem rev. 2014;114(24):12278-12329;Available from: https://doi.org/10.1021/cr4005499.
3. Duy TT, Sawada SI, Hasegawa S, Katsumura Y, Maekawa Y. Poly (ethylene-co-tetrafluoroethylene)(ETFE)-based graft-type polymer electrolyte membranes with different ion exchange capacities: relative humidity dependence for fuel cell applications. J Membr Sci. 2013;447:19-25;Available from: https://doi.org/10.1016/j.memsci.2013.07.041.
4. Hao LH, Hieu DTT, Luan LQ, Phuong HT, Dinh VP, Tuyen LA, Hong PTT, Man TV, Tap T D. Electron and gamma irradiation-induced effects in poly (ethylene-co-tetrafluoroethylene) films. J. Appl. Polym. Sci. 2022;139(29):e52620;Available from: https://doi.org/10.1002/app.52620.
5. Tap TD, Sawada SI, Hasegawa S, Yoshimura K, Oba Y, Ohnuma M, Katsumura Y, Maekawa Y. Hierarchical structure-property relationships in graft-type fluorinated polymer electrolyte membranes using small- and ultrasmall-angle X-ray scattering analysis. Macromolecules. 2014;47(7):2373-83;Available from: https://doi.org/10.1021/ma500111x.
6. Tap TD, Nguyen LL, Hien NQ, Thang PB, Sawada SI, Hasegawa S, Maekawa Y. Humidity and temperature effects on mechanical properties and conductivity of graft-type polymer electrolyte membrane. Radiat Phys Chem. 2018;151:186-191;Available from: https://doi.org/10.1016/j.radphyschem.2018.06.033.
7. Tap TD, Nguyen LL, Zhao Y, Hasegawa S, Sawada SI, Hung NQ, Tuyen LA, Maekawa Y. SAXS Investigation on morphological change in lamellar structures during propagation steps of graft-type polymer electrolyte membranes for fuel cell applications. Macromol Chem Phys. 2020;221(3):1900325;Available from: https://doi.org/10.1002/macp.201900325.
8. Tap TD, Nguyen LL, Hasegawa S, Sawada SI, Luan LQ, Maekawa Y. Internal and interfacial structure analysis of graft-type fluorinated polymer electrolyte membranes by small-angle X-ray scattering in the high-q range. J Appl Polym Sci. 2020;137(35):49029;Available from: https://doi.org/10.1002/app.49029.
9. Hao LH, Tap TD, Hieu DTT, Korneeva E, Tiep NV, Yoshimura K, Hasegawa S, Sawada SI, Man TV, Hung NQ, Tuyen LA, Phuc DV, Luan LQ, Maekawa Y. Morphological characterization of grafted polymer electrolyte membranes at a surface layer for fuel cell application. J Appl Polym Sci. 2022;139(14):51901;Available from: https://doi.org/10.1002/app.51901.
10. Hieu DTT, Hao LH, Long TH, Tien VV, Cuong NT, Man TV, Loan TTH, Tap TD. Investigation of chemical degradation and water states in the graft-type polymer electrolyte membranes.

Polym Eng Sci. 2022;62(9):2757-2768;Available from: https://doi.org/10.1002/pen.26059.
11. Long TH, Hieu DTT, Hao LH, Cuong NT, Loan TTH, Man TV, Tap TD. Positron annihilation lifetime spectroscopic analysis of nafion and graft-type polymer electrolyte membranes for fuel cell application. Polym Eng Sci. 2022;62(12):4005-4017;Available from: https://doi.org/10.1002/pen.26162.
12. Tap TD, Long TH, Hieu DTT, Hao LH, Phuong HT, Luan LQ, Man TV. Positron annihilation lifetime study of subnano level free volume features of grafted polymer electrolyte membranes for hydrogen fuel cell applications. Polym Adv Technol. 2022;33(9):2952-2965;Available from: https://doi.org/10.1002/pat.5761.
13. Tap TD, Hasegawa S, Yoshimura K, Yen VTK, Tue NHM, Tuan NM, Hieu DTT, Tuan HA, Hao HL, Nguyen LL, Phuong HT, Luan LQ, Man TV, Maekawa Y. Phase separation and water channels in graft-type polymer electrolyte membranes for hydrogen fuel cell. Int J Hydrog Energy. 2024;59:777-790;Available from: https://doi.org/10.1016/j.ijhydene.2024.02.082.
14. Dinh TTH, Lam HH, Tran TD, Le QL, Huynh TP, Luu AT, Pham KN, Tran DT. FT-IR analysis of the water states of the poly(styrene sulfonic acid)-grafted poly(ethylene-co-tetrafluoroethylene) copolymer. Minist Sci Technol Vietnam. 2022;64(2):3-9;Available from: https://doi.org/10.31276/VJSTE.64(2).03-09.
15. Hieu ĐTT, Hao LH, Danh TT, Long TH, Cuong NT, Man TV, Loan TTH, Tap TD. Study on the mechanism of graft polymerization and sulfonation of proton exchange membranes for fuel cell. VJST B. 2022;64(6);Available from: https://b.vjst.vn/index.php/ban_b/article/view/1282.
16. Tue NHM, Long TH, Hieu DTT, Hao LH, Yen VTK, Tuan NM, Phuong HT, Luan LQ, Hong PTT, Man TV, Tap TD. Effects of source correction on positron annihilation lifetime spectroscopic analysis of graft-type polymer electrolyte membranes. Sci Technol Dev J. 2023;26(4):press-press;Available from: https://doi.org/10.32508/stdj.v26i4.4052.
17. Tap TD. Study on the structures of polymer electrolyte membrane for fuel cell applications using small and ultrasmall angle X-ray scattering. VJST B. 2018;60(8):8-11;Available from: https://b.vjst.vn/index.php/ban_b/article/view/624.
18. Nguyen LL, Hao LH, Hai LV, Ngan NNK, Cuong NT, Tuyen LA, Phuc PT, Phuong HT, Luan LQ, Hue NTN, Tap TD. Application of small-angle X-ray scattering to evaluate the impact of electron density fluctuation on the micro structures of proton exchange membrane in fuel cell. VJST B. 2020;62(1);Available from: https://b.vjst.vn/index.php/ban_b/article/view/941.
19. Lam HH, Dinh TTH, Tran HL, Dang VH, Tran TD, Tran VM, Le QL, Huynh TP, Pham TTH, Tran DT. Investigation of the lamellar grains of graft-type polymer electrolyte membranes for hydrogen fuel cell application using ultrasmall-angle X-ray scattering. VNU J Sci Nat Sci Technol. 2021;37(4);Available from: https://doi.org/10.25073/2588-1140/vnunst.5216.
20. Yen VTK, Hieu DTT, Hao LH, Long TH, Tue NHM, Tuan NM, Cuong NT, Loan TTH, Man TV, Tap TD. Characterization of graft-type polymer electrolyte membranes at low grafting degrees for fuel cells. Sci Technol Dev J. 2023;26(2):2799-2807;Available from: https://doi.org/10.32508/stdj.v26i2.4051.
21. Hao LH, Hieu DTT, Danh TT, Long TH, Phuong HT, Man TV, Tuyen LA, Ngoc PK, Tap TD. Surface features of polymer electrolyte membranes for fuel cell applications: an approach using S2p XPS analysis. Sci Technol Dev J. 2021;24(3):2100-2109;Available from: https://doi.org/10.32508/stdj.v24i3.2556.
22. Zhao Y, Yoshimura K, Sawada S, Motegi T, Hiroki A, Radulescu A, Maekawa Y. Unique structural characteristics of graft-type proton-exchange membranes using SANS partial scattering function analysis. Macromolecules. 2022;55(16):7100-7109;Available from: https://doi.org/10.1021/acs.macromol.2c00333.
23. Balog S, Gasser U, Mortensen K, Gubler L, Scherer GG. Nanoscale morphology in graft copolymer proton-exchange membranes cross-linked with DIPB. J Membr Sci. 2011;383(1-2):50-59;Available from: https://doi.org/10.1016/j.memsci.2011.08.031.
24. Ding YS, Hubbard SR, Hodgson KO, Register RA, Cooper SL. Anomalous small-angle X-ray scattering from a sulfonated polystyrene ionomer. Macromolecules. 1988;21(6):1698-1703;Available from: https://doi.org/10.1021/ma00184a028.
25. Nishikawa K, Kasahara Y, Ichioka T. Inhomogeneity of mixing in acetonitrile aqueous solution studied by small-angle X-ray scattering. J Phys Chem B. 2002;106(3):693-700;Available from: https://doi.org/10.1021/jp011964v.
26. Amann M, Diget JS, Lyngsø J, Pedersen JS, Narayanan T, Lund R. Kinetic pathways for polyelectrolyte coacervate micelle formation revealed by time-resolved synchrotron SAXS. Macromolecules. 2019;52(21):8227-8237;Available from: https://doi.org/10.1021/acs.macromol.9b01072.
27. Teubner M, Strey R. Origin of the scattering peak in microemulsions. J Chem Phys. 1987;87(5):3195-3200;Available from: https://doi.org/10.1063/1.453006.
28. Schubert KV, Strey R, Kline SR, Kaler EW. Small angle neutron scattering near Lifshitz lines: transition from weakly structured mixtures to microemulsions. J Chem Phys. 1994;101(6):5343-5355;Available from: https://doi.org/10.1063/1.467387.
29. Endo H, Mihailescu M, Monkenbusch M, Allgaier J, Gompper G, Richter D, Jakobs B, Sottmann T, Strey R, Grillo I. Effect of amphiphilic block copolymers on the structure and phase behavior of oil-water-surfactant mixtures. J Chem Phys. 2001;115(1):580-600;Available from: https://doi.org/10.1063/1.1377881.
30. Putnam CD, Hammel M, Hura GL, Tainer JA. X-ray solution scattering (SAXS) combined with crystallography and computation: defining accurate macromolecular structures, conformations and assemblies in solution. Q Rev Biophys. 2007;40(3):191-285;Available from: https://doi.org/10.1017/S0033583507004635.
31. Grady BP, Matsuoka H, Nakatani Y, Cooper SL, Ise N. Influence of the sample preparation method of the ultrasmall-angle X-ray scattering of lightly sulfonated polystyrenes. Macromolecules. 1993;26(15):4064-4066;Available from: https://doi.org/10.1021/ma00067a055.
32. Zhang F, Ilavsky J, Long GG, Quintana JP, Allen AJ, Jemian PR. Glassy carbon as an absolute intensity calibration standard for small-angle scattering. Metall Mater Trans A. 2010;41:1151-1158;Available from: https://doi.org/10.1007/s11661-009-9950-x.
33. Habicht A, Schmolke W, Goerigk G, Lange F, Saalwaechter K, Ballauff M, Seiffert S. Critical fluctuations and static inhomogeneities in polymer gel volume phase transitions. J Polym Sci B: Polym Phys. 2015;53(16):1112-1122;Available from: https://doi.org/10.1002/polb.23743.
34. Shi C, Liu T, Chen W, Cui F, Liu L, Cai Y, Li Y. Interaction, structure and tensile property of swollen nafion membranes. Polymer. 2021;213:123224;Available from: https://doi.org/10.1016/j.polymer.2020.123224.
35. Woo E, Coletta E, Holm A, Mun J, Toney MF, Yoon DY, Frank CW. Polyimide-PEG segmented block copolymer membranes with high proton conductivity by improving bicontinuous nanostructure of ionic liquid-doped films. Macromol Chem Phys. 2019;220(9):1900006;Available from: https://doi.org/10.1002/macp.201900006.
36. Shiino K, Otomo T, Yamada T, Arima H, Hiroi K, Takata S, Miyake J, Miyatake K. Structural investigation of sulfonated polyphenylene ionomers for the design of better performing proton-conductive membranes. ACS Appl Polym Mater. 2020;2(12):5558-5565;Available from: https://doi.org/10.1021/acsapm.0c00895.
37. Balog S, Gasser U, Mortensen K, Gubler L, Scherer GG. Nanoscale morphology in graft copolymer proton-exchange membranes cross-linked with DIPB. J Membr Sci. 2011;383(1-2):50-59;Available from: https://doi.org/10.1016/j.memsci.2011.08.031.